# Pattern formation and interface pinch-off in rotating Hele-Shaw flows: A phase-field approach

R. Folch,[1] E. Alvarez-Lacalle,[2] J. Ortín,[3] and J. Casademunt[3]
[1]*Departament d'Enginyeria Química, Universitat Rovira i Virgili, Av. dels Països Catalans 26, E-43007 Tarragona, Spain*
[2]*Departament de Física Aplicada, Universitat Politècnica de Catalunya, Av. Dr. Gregorio Marañón 50, E-08028 Barcelona, Spain*
[3]*Departament ECM, Universitat de Barcelona, Av. Diagonal 647, E-08028 Barcelona, Spain*
(Received 17 February 2009; revised manuscript received 29 July 2009; published 16 November 2009)

Viscous fingering dynamics driven by centrifugal forcing is studied for arbitrary viscosity contrast. Theoretical methods, including exact solutions, and numerics based on a phase-field approach are used. Both confirm that pinch-off singularities in patterns originated from the centrifugally driven instability may occur spontaneously and be inherent to the two-dimensional Hele-Shaw dynamics. They are systematically more frequent for lower viscosity contrasts consistently with experimental evidence. The analytical insights provide an interpretation of this fact in terms of the asymptotic matching of the different regions of the fingering patterns. The phase-field numerical scheme is shown to be particularly adequate to elucidate the existence of finite-time singularities through the dependence of the singularity time on the interface thickness, in particular for varying viscosity contrast.

DOI: 10.1103/PhysRevE.80.056305 PACS number(s): 47.15.gp, 47.20.Ma, 47.55.df, 47.11.−j

## I. INTRODUCTION

Topological singularities such as interface pinch-off in fluid flows have been the object of intense study in the last decades [1–12]. The unavoidable breakdown of the hydrodynamic description of a thin fluid filament at pinch-off is reflected in the spontaneous generation of singular behavior at a finite time. In the neighborhood of such singularities the problem might become scale-free giving rise to self-similar scaling behavior for which some degree of universality is naturally expected [1]. Interestingly, a continuum hydrodynamic description may correctly predict the occurrence of finite-time singularities out of a smooth initial condition and be continued uniquely through the singularity even though it may not implement the interface breakup and reconnection, which necessarily involves microscopic physics. This is the case, for instance, of three-dimensional (3D) jets [1].

In contrast to the case of 3D fluid filaments, two-dimensional (2D) filaments are not linearly unstable under capillary forces alone and their dynamics may be more involved and less universal. Interface breakup has been studied in 2D Stokes flow [5] and in particular in the case of Hele-Shaw (H-S) flows, a paradigmatic system in fluid dynamics and pattern formation [13–16]. It is well known that the 2D H-S dynamics can lead to finite-time pinch-off [6,7]. Surface tension alone has been shown to drive a configuration of two droplets of fluid connected by a neck to finite-time pinch-off in two-dimensional simulations for initial conditions sufficiently close to pinch-off [11,12]. A thin fluid filament can also be made to pinch at finite time under some specific boundary conditions [6–10].

Here we will address the case of centrifugally-driven viscous fingering in H–S cells [17–20], a setup which is particularly interesting from the perspective of pinch-off singularities for two main reasons. First, because in this problem configurations close to pinch-off appear naturally as the generic asymptotic evolution after a morphological instability starting from initial conditions arbitrarily distant from such pinching morphologies. This is in contrast to most previous studies, where the focus was on the local self-similar structure of the singularities and the occurrence of the singularities was rather induced by the choice of initial or boundary conditions. The second reason is that the singularities generated in this setup result from the competition of capillary vs centrifugal forces and the self-similar nature of the singularities themselves is likely to be inherently different from the cases studied before driven solely by capillary forces. This second point will not be addressed here. Our main focus will be on the dynamics of the approach to pinch-off and specifically on whether the singularities occur at finite time. In particular we will be interested in elucidating the connection between the singularities of the 2D H-S problem and those observed in experiments, which unavoidably include spurious 3D effects.

(i) Viscosity contrast: the viscosity Atwood ratio of the two fluids, or viscosity contrast $A$, has been shown to have strong nontrivial effects on the nonlinear dynamics of fingering patterns in general [15,21,22]. For pinching phenomena in particular, in 3D it is known that this parameter has a strong influence on the interface shape near pinching [23]. In 2D H-S flows, the situation is quite involved. Experiments of air displacing a liquid in a channel geometry ($A=1$) show that fingers formed in the viscosity-driven morphological instability compete until a single finger is left [13], but the necks of the transient and final fingers do not pinch. In contrast, when a denser liquid displaces a second less dense liquid of similar viscosity (typically $A \simeq 0-0.5$) in a tilted channel, the density-driven morphological instability gives rise to fingers that now do not compete as efficiently as for high viscosity contrast but elongate to form thin filaments with a droplet at their tip [22] which can indeed pinch off [21]. From those results one could be tempted to correlate the dependence of the pinch-off frequency on $A$ to the occurrence of thin filaments (which is indeed sensitive to $A$). The rotating setup, however, produces elongated thin fingers regardless of $A$. In this case, the experimental evidence shows that indeed pinch-off events occur much more often and systematically for low $A$ (two liquids) than for high $A$ (liquid and air).

 ©2009 The American Physical Society

(ii) Intrinsic vs extrinsic singularities: a fundamental question that underlies the present discussion, and the connection between the effective 2D description of the system and the real experiments, concerns the role of the cell gap as a natural cutoff length scale in the problem. The usual H-S model is based on the fact that, for sufficiently small $b$ (low Reynolds number limit) the problem can be formally projected into an effective 2D description provided that the flows are not resolved at scales comparable to the cell gap $b$. We refer to this standard description of flows in H-S cells as the 2D Hele-Shaw model. The actual pinch-off of a fluid filament in our system, however, will unavoidably cross this limit of validity of the 2D description when the distance between the two approaching interfaces is comparable or smaller than $b$. Therefore, other effects associated to the actual 3D structure of the interface will necessarily be present at pinch-off in any physical realization of our system in a Hele-Shaw cell. A central point in our present discussion is to elucidate whether and when the pinch-off singularities may be *intrinsic* (inherent to the 2D H-S model) or *extrinsic* (associated to 3D effects, not contained in the 2D H-S model). In the latter case, the occurrence of singularities could be potentially modified by changing the experimental conditions while keeping $A$ and dimensionless surface tension $B$ fixed (for instance delayed by decreasing $b$). Similarly, the systematic difference on pinch-off events observed between experiments with an air-liquid interface and those with two liquids could be due either to the difference in wetting conditions or inherent to the difference of viscosity contrast $A$. This point has clear experimental relevance but is very difficult to elucidate experimentally. Discriminating on the extrinsic vs intrinsic nature of the singularities in the 2D H-S model from numerical simulations could certainly clarify the issue.

(iii) Phase-field approach: the precise analysis of the pinch-off singularities by numerical means is usually done in the so-called lubrication approximation. The problem is inherently nonlinear and is known to be very delicate and numerically demanding, in particular for 2D, even if the lubrication approximation renders the problem local, as for $A=1$ [11,12]. This strategy is applied to the case of rotating H-S flows with $A=1$ in the accompanying paper, Ref. [24]. However, for $A<1$, the lubrication approximation is nonlocal and the problem has a higher level of difficulty [24]. Therefore, for arbitrary $A$ we propose an alternative approach based on a diffuse-interface (i.e., phase-field) description of the problem, which can handle equally well any viscosity contrast. Phase-field modeling has been successfully applied to a variety of interfacial problems as a powerful alternative to sharp-interface, boundary-integral methods (see, for example, [25–27]), in particular for Hele-Shaw flows [28–30], at the price of introducing a new length scale, the finite thickness of the interface. This regularizes the pinch-off singularities and provides an *ad hoc* mechanism of interface recombination that allows to continue the dynamics through the topological change. For the present discussion, however, it is appealing that the existence of such cutoff does mimic the role of the real cutoff length $b$ of the H-S model. Indeed, we will turn the dependence of pinch-off time on the cutoff into a tool to explore the existence of finite-time singularities in the 2D model. In this spirit, our approach is closer to an experimental point of view, where one would like to control separately, on the one hand, the two dimensionless parameters $A$ and $B$ of the 2D H-S model, and on the other hand, the cutoff $b$. A second reason to use phase-field modeling is that the numerical simulation turns out to be much simpler than sharp-interface methods, in particular, if $A$ is to be changed arbitrarily [27–29].

Consistently with experiments, we find that singularities occur more frequently for low $A$ and seem to be intrinsic in this parameter range (for more general settings than those originally studied in Refs. [6–12]). Remarkably, the phase-field approach is conclusive in this case (which is most demanding for sharp-interface methods) but not quite for high viscosity contrast ($A=1$). Fortunately, the latter is more amenable to sharp-interface methods as presented in Ref. [24], where it is shown that, while finite-time singularities may exist in the appropriate circumstances for $A=1$, they do not exist when centrifugal forces are dominant—in situations where singularities actually occur for $A<1$.

(iv) Layout: Sec. II briefly reviews the existing experimental evidence and defines the mathematical formulation of the problem. In Sec. III we discuss the theoretical framework and some analytical insights. Phase-field simulations are presented and discussed in Sec. IV and conclusions are summarized in Sec. V.

## II. PROBLEM

### A. Setup and physical parameters

Our specific H-S setup consists of two parallel horizontal plates with a small gap $b$ in between. The cell spins around its vertical axis at constant angular velocity $\Omega$. A drop of a liquid of density $\rho_{\text{in}}$ occupies the inner region of the cell, while a second less dense fluid occupies the outer region ($\rho_{\text{out}}<\rho_{\text{in}}$). Initially the inner drop is centered with the rotation axis and has an approximately circular shape of radius $R_0$. If the centrifugal forcing is strong enough to overcome capillary forces, the circular shape is unstable leading to viscous fingering patterns. The fingers are stretched by the centrifugal forcing and, thus, evolve into elongated thin filaments with a drop at the end. The problem depends on two dimensionless parameters, the viscosity contrast

$$A = \frac{\mu_{\text{in}} - \mu_{\text{out}}}{\mu_{\text{in}} + \mu_{\text{out}}}, \tag{1}$$

where $\mu_{\text{in}}$ and $\mu_{\text{out}}$ are the dynamic viscosities of the inner and outer fluids, respectively, and the dimensionless surface tension

$$B = \frac{\sigma}{\Delta\rho\Omega^2 R_0^3}, \tag{2}$$

where $\Delta\rho=\rho_{\text{in}}-\rho_{\text{out}}$, which measures the relative strength of capillary to centrifugal forces.

### B. Previous experimental evidence

We briefly recall the main experimental results on rotating Hele-Shaw flows relevant to the present study. They were

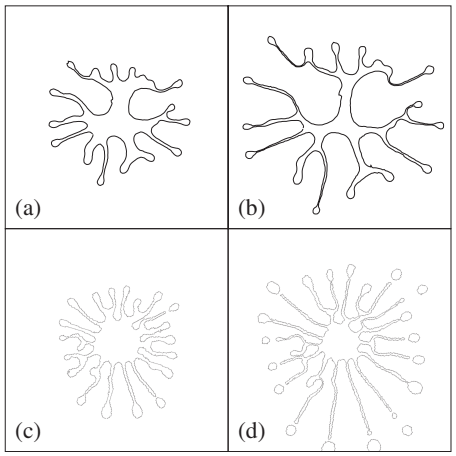


FIG. 1. Pattern evolution for $A=1$, $b=0.5$ mm, $\Omega=120$ rev/min, and $R_0=50$ mm (a,b), and $A\simeq 0.45$, $\Omega=180$ rev/min, and $R_0=38$ mm (c,d). Snapshots of size $3R_0\times 3R_0$ are shown at times 16.5 s (a), 22.5 s (b), 122 s (c), and 158 s (d) after the cell was set in rotation.

described and discussed extensively in Refs. [17,19,31] for both high and low viscosity contrasts. Figures 1(a,b) and 1(c,d) show the typical patterns formed at two different stages, for high ($A=1$) and low ($A\simeq 0.45$) viscosity contrast, respectively. While the whole range of $A$ could not be spanned, additional numerical evidence shows that the dynamics is quite insensitive to $A$ for most of the range, except very close to $A=1$, where a different behavior sets in. This has been discussed in Refs. [16,19,32]. This observation applies also for pinching phenomena, where the frequency of singularities depends only weakly on $A$, except very close to $A=1$, so we essentially distinguish two types of behavior, the high-contrast case $A=1$, and the low-contrast case, for most of the range $A<1$. It is worth mentioning that the experimental results for $A=1$, with silicone oil displacing air, were all performed with prewetted cells to avoid contact-line dynamic effects. With prewetted cells, the $A=1$ dynamics is closest to the standard 2D Hele-Shaw model as discussed in Ref. [31].

In addition to some morphological differences, mostly concerning the fingers of the outer fluid penetrating the inner one [33], the most striking difference between low and high viscosity contrast experiments is the systematic droplet pinch-off observed for $A\simeq 0.45$ and not for $A=1$. For the latter, filaments keep on stretching until they reach a width comparable to the cell gap thickness with very rare pinch-off in the observable time.

### C. 2D free-boundary problem

The standard Hele-Shaw free-boundary problem is defined by the incompressibility condition $\vec{\nabla}\cdot\vec{v}_i=0$, where $\vec{v}_i$ is the 2D averaged velocity field in fluid $i$, together with the continuity of normal velocity across the interface and the tangential velocity jump as boundary conditions. We write down the problem in dimensionless variables by measuring lengths in units of the initial drop radius $R_0$ and time in units of $t^*=12(\mu_{\rm in}+\mu_{\rm out})/b^2\Omega^2\Delta\rho$.

It is convenient for the phase-field approach to use the formulation in terms of the stream function $\psi$ defined through $\vec{u}=\vec{\nabla}\times\psi\hat{z}$ (where $\vec{u}$ is now the dimensionless fluid velocity and $\hat{z}$ is the direction perpendicular to the plates). The stream function is harmonic but, contrary to the pressure field, $\psi$ is continuous across the interface. In terms of the stream function the free-boundary problem is fully specified by the following governing equations [15,30]:

$$\nabla^2\psi=0, \tag{3a}$$

$$\partial_s\psi|_{\rm in}=\partial_s\psi|_{\rm out}=-u_n, \tag{3b}$$

$$\partial_n\psi|_{\rm out}-\partial_n\psi|_{\rm in}=\Gamma, \tag{3c}$$

where $s$ and $n$ are coordinates tangential and normal to the interface, respectively. The magnitude of the tangential velocity jump is the strength $\Gamma$ of the (singular) vorticity at the interface, $\Gamma\equiv\gamma+A(\partial_n\psi|_{\rm in}+\partial_n\psi|_{\rm out})$, where $\gamma/2\equiv(B\vec{\nabla}\kappa-\vec{r})\cdot\hat{s}$ is its local part, with $\kappa$ being the in-plane curvature ($\kappa>0$ for a circle) and $\vec{r}$ the radial coordinate. The explicit form of the vorticity is what defines specifically the case with rotation formulated in the corotating frame [17].

### D. Phase-field model

Here we present the phase-field model for rotating H-S flows, as a direct extension of the one presented in Refs. [28,29], with the corresponding modification of the vorticity at the interface to account for the centrifugal forcing:

$$\tilde{\epsilon}\frac{\partial\psi}{\partial t}=\nabla^2\psi+A\vec{\nabla}\cdot(\theta\vec{\nabla}\psi)+\frac{1}{\epsilon}\frac{1}{2\sqrt{2}}\gamma(\theta)(1-\theta^2), \tag{4a}$$

$$\epsilon^2\frac{\partial\theta}{\partial t}=f(\theta)+\epsilon^2\nabla^2\theta+\epsilon^2\kappa(\theta)|\vec{\nabla}\theta|+\epsilon^2\hat{z}\cdot(\vec{\nabla}\psi\times\vec{\nabla}\theta), \tag{4b}$$

where $\theta$ is the phase field, an auxiliary field distinguishing between the two fluids, $f(\theta)\equiv\theta(1-\theta^2)$, $\gamma(\theta)/2\equiv\hat{s}(\theta)\cdot[B\vec{\nabla}\kappa(\theta)-\vec{r}]$, and $\kappa(\theta)\equiv-\vec{\nabla}\cdot\hat{n}(\theta)$, with $\hat{n}(\theta)\equiv\vec{\nabla}\theta/|\vec{\nabla}\theta|$ and $\hat{s}(\theta)\equiv\hat{n}(\theta)\times\hat{z}$.

Apart from the physical control parameters $A$ and $B$, the dynamics in this model also depends on an artificial interface thickness $\epsilon$ and a relaxation time for the stream function $\tilde{\epsilon}$ which may be taken in general as different for numerical convenience. In the limit $\epsilon,\tilde{\epsilon}\to 0$, the dynamics is strictly that of Eqs. (3a)–(3c). Convergence with $\epsilon,\tilde{\epsilon}$ was discussed in Ref. [29].

## III. THEORETICAL ANALYSIS

### A. Asymptotics

Before analyzing our numerical results, it is useful to define the theoretical framework that arises from a series of analytical results on the asymptotics of different regions of the pattern. We will see that some analytical insights help us understand in simple physical terms the formation of singu-

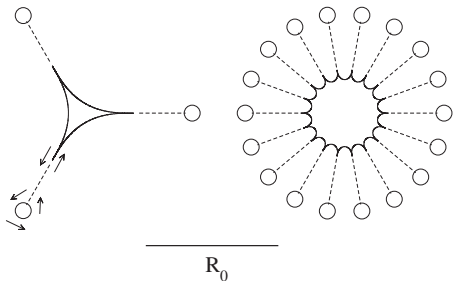


FIG. 2. Asymptotic shapes of different regions of the $n$-fold symmetric pattern for $n=3$ and $n=18$: central region, starfish (stationary) solutions; dashed lines, infinitely thin filaments (lubrication region); circles, outer solution tending to circular droplets moving infinitely apart with an exponential velocity. Arrows indicate the direction of the arclength coordinate.

larities and reinforce the strength of the conclusions from the numerics.

The long time regime emerging from the morphological instability of a nearly circular interface consists of long and thin filaments ended in a nearly circular droplet that accelerates away from the cell center, while a fraction of the mass of the initial circle is trapped around the axis. For a perfectly symmetric $n$-folded configuration the physical picture is schematically depicted in Fig. 2. Three different regions may be distinguished according to their asymptotics. First is a central region of finite area that tends to a stationary shape with cusplike protrusions which connect with the fluid filaments. This region around the cell axis will be referred to as the *inner region*. The *lubrication region* will be that of the long and thin fluid filament, depicted as dashed lines in Fig. 2, which is governed by the lubrication approximation and where the pinch-off singularities may possibly occur. Finally, we will refer to the *outer region* as the one closing the fluid filaments with nearly circular droplets of finite area, which accelerate exponentially away. The asymptotics of the three regions can be analytically studied separately. While the matching conditions have to be worked out carefully and may in general be nontrivial, as discussed in Ref. [24] for $A=1$, we will see that for low $A$ the lowest-order asymptotics already yields interesting clues on a possible mechanism of singularity formation.

### B. Inner region: starfish solutions

The asymptotics of the inner region of a $n$-fold symmetric pattern (for $n>2$) is governed by what we call starfish solutions (see Fig. 2). These are stationary shapes, where capillary forces balance exactly centrifugal forces. These shapes are independent of $A$ and must satisfy the condition of zero vorticity,

$$\sigma\partial_s\kappa = \Delta\rho\Omega^2\vec{r}\cdot\hat{s}. \tag{5}$$

Similar classes of solutions were reported in Ref. [34]. Our starfish solutions are fundamentally different in that the above equation is fulfilled only piecewise, thus, allowing for boundary conditions that involve cusps. Remarkably, these solutions are stable with respect to perturbations preserving the $n$-fold symmetry, in contrast to those of Ref. [34], which are continuous but change concavity and are unstable. The smooth matching to the lubrication region removes the cusps and requires $\kappa\to 0$ at the cusps of the starfish solutions. The physical interpretation of the cusp is that the two sides must be continued as two superposed radial straight lines which can be connected at infinity in any smooth nonsingular shape.

It is interesting to realize that, as an attractor of the dynamics for the $n$-fold symmetric subspace, these solutions exhibit a different topology from the initial condition (the solution consists of $n$ disconnected arcs with $n$ missing points at the cusps) clearly evoking the existence of topological singularities at least at infinite time. We have explicitly checked the approach to these solutions in our phase-field simulations (results not shown). For nonsymmetric initial conditions, these solutions have still some relevance as saddle points of the dynamics explaining the transient slowing down observed in multifinger experiments [19].

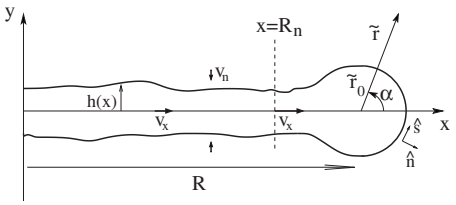


FIG. 3. Sketch of a filament of fluid with a droplet at its tip.

### C. Scaling of the lubrication region

To analyze the asymptotics of a thin radial filament (Fig. 3) we rely on the lubrication approximation. This has been derived in detail for the present problem in Ref. [24]. For the height $h(x,t)$ of the interface along a radial coordinate $x$, this reads

$$\frac{1+A}{2}\partial_t h = -\partial_x(xh) - B\partial_x(h\partial_x^3 h) - \frac{1-A}{1+A}\partial_x(h\mathcal{H}[\partial_x(xh)]), \tag{6}$$

where the integral operator $\mathcal{H}$ is a Hilbert transform. Note that the two relevant parameters $A$ and $B$ appear associated to different terms. The first term in the right-hand side accounts for the centrifugal force and is the lowest-order contribution in the lubrication expansion [35]. The two other terms constitute the next to leading order contributions. The local term associated to capillarity $B$ is exactly the same as for the purely capillary driven case, while the nonlocal one is associated to viscosity contrast $A$. Note that the case $A=1$ is manifestly special in that the lubrication approximation remains local.

We define the basic scaling of the filaments as that provided by the lowest order of the lubrication approximation and will address later how the effect of the other terms may modify these asymptotics. Keeping only this first term in the right-hand side of Eq. (6), any given initial condition $h_0(x)$ evolves following the simple scaling $h(x,t)=L(t)h_0[L(t)x]$, with $L(t)=e^{-K't}$ and $K'=2/(1+A)$. This implies that, in gen-

eral, any *radial* fluid filament should stretch and narrow to produce pinch-off at least at infinite time. Note that the dependence on $A$ here is an artifact of the chosen dimensionless units. In fact, the characteristic time scale of this exponential scaling is $t'=12\mu_{\text{in}}/b^2\Omega^2\Delta\rho$ so that it only depends on the viscosity of the inner fluid because to lowest order the problem is decoupled from the outer fluid. As we will see, this point will have consequences for the matching with the outgoing droplet at the end of the filament.

### D. Outer region: droplet solutions

To complete the analysis we must check if the nearly circular droplet that closes the filament of fluid may be asymptotically approaching some other attractor of the dynamics. We find that an isolated, circular, off-center droplet is an exact solution for arbitrary $A$, which preserves its circular shape provided the distance of its center to the rotation axis grows exponentially as $R(t)=R(0)e^{Kt}$, with $K=1$. This can be proved by transforming the equations of motion into the reference frame of the droplet center. The vorticity $\Gamma$ in that frame gets an additional term of the form $(1-A)R(t)\hat{x}\cdot\hat{s}$. The case $A=1$, first reported in Ref. [36], becomes trivial, since the equations are fully invariant with respect to this change. This implies that all the dynamics, including the nonlinear regime, are exactly mapped. For $A<1$, instead, the evolution of the shape of a perturbed circle at the cell center or initially away from it is no longer the same. Nevertheless, one can prove that a circle exponentially moving off center is also an exact solution with the same rate $K=1$, with a nontrivial velocity field of the form

$$\vec{u}_{\text{in}}=\dot{R}\hat{x}, \tag{7a}$$

$$\vec{u}_{\text{out}}=\dot{R}(r_0/r')^2(\hat{x}\cos 2\alpha+\hat{y}\sin 2\alpha), \tag{7b}$$

where $r_0$ is the radius of the droplet and $r',\alpha$ are polar coordinates centered at the droplet (see Fig. 3).

Note that the isolated droplet moves exponentially with a characteristic time scale $t^*=12(\mu_{\text{in}}+\mu_{\text{out}})/b^2\Omega^2\Delta\rho$ that depends on the viscosity of the outer fluid that must be dragged, while the lubrication region scales exponentially (to lowest order) with the characteristic time $t'=12\mu_{\text{in}}/b^2\Omega^2\Delta\rho$, which involves only the inner fluid viscosity. The mismatch between these two time scales is at the root of the qualitative distinction between $A=1$ and $A<1$. The scaling of the thinning/stretching of the radial filaments actually expresses mass conservation, so the fact that for $A=1$ the exponential rate exactly coincides with the asymptotic velocity of the droplet at the end suggests that a "smooth" matching is plausible. On the contrary, the mismatch of time scales for $A<1$ suggests that the mass expelled at the end of the filament cannot be smoothly absorbed in the displacement of a stationary droplet so that a singularity is likely to build up. This yields a simple intuitive physical explanation of why one may expect a different behavior for $A=1$ and $A<1$ as far as finite-time singularities are concerned. A more precise analysis of this matching for $A=1$ is performed in Ref. [24].

## IV. NUMERICAL RESULTS

### A. Numerical procedure

We numerically integrate the phase-field model using a forward-time-centered-space scheme. The time step $dt$ is taken to be close to the stability limit: $dt=0.2\tilde{\epsilon}dx^2$, where $dx$ is the mesh spacing. We have tested that a smaller $dt$ does not affect the results. Convergence of the solution is also tested changing $dx$ ($dx=\epsilon$ generally suffices as shown in [29]). For reliable quantitative comparison with theory and experiments, we also check convergence of the time constant $K$ in $\epsilon$ and $\tilde{\epsilon}$, since $\tilde{\epsilon}$ conveys some finite diffusion time to the flow and $\epsilon$ delays the interface advance with respect to the normal fluid velocities [28]. A value of $\tilde{\epsilon}=0.5$ turns out to guarantee accurate results. Convergence in $\epsilon$ is more cumbersome and it is checked case by case.

Our initial condition is some perturbation of a centered circle of unit radius, $r=1+\Delta r(\varphi)$, where $r$ and $\varphi$ are polar coordinates with respect to the rotation axis and $\Delta r(\varphi)\ll 1$. In the following subsections, except for Sec. IV B, we consider only identical fingers ($n$-fold symmetry), $\Delta r(\varphi)=(2\pi/n)q\cos(n\varphi)$, where $q$ is the amplitude to wavelength ratio of the perturbation and $n$ is the (integer) number of fingers. Unless otherwise stated, we use $q=0.05$ and a dimensionless surface tension $B$ for which $n$ is the most unstable mode in the linear regime except for the case $n=2$, $B=0.01$, and $q=0.2$ in Figs. 6 and 7, where a smaller dimensionless surface tension is purposely tested.

### B. Qualitative comparison with experiments

In order to compare with the patterns shown in Fig. 1, which have 15–16 filaments for $A=1$ [Figs. 1(a) and 1(b)] and 20–21 for $A\simeq 0.45$ [Figs. 1(c) and 1(d)], we use a dimensionless surface tension $B=1.03\times 10^{-3}$, which corresponds to a most unstable mode $n=18$. We use exactly the same initial condition and physical and computational parameters for both high and low viscosity contrasts, so that the effects of $A$ can be clearly isolated. The initial condition for the simulation has been chosen to reproduce only roughly the specific initial conditions of the corresponding experiments depicted in Fig. 1. Finally, we take the less refined choices $dx=\epsilon$ and $\tilde{\epsilon}=1$ with an interface thickness down to $\epsilon=0.005$ in order to avoid possible spurious pinch-off events. As we will see for the dumbbell-shaped patterns in Sec. IV C, we find that, whenever pinch-off occurs, a lower value of the ratio $dx/\epsilon$ does not prevent it but rather anticipates it. Figure 4 is to be qualitatively compared to its experimental counterpart of Fig. 1. Patterns are shown at two different times: $t=1.32$ (left) and $t=1.74$ (right) for three different viscosity contrasts. The snapshots correspond to the times when the pattern envelope has roughly attained twice [Figs. 1(a) and 1(c) and Figs. 4(a), 4(c), and 4(e)] and three times [Figs. 1(b) and 1(d) and Figs. 4(b), 4(d), and 4(f)] the initial radius.

Let us first compare patterns at the earlier stage [Fig. 1(a) with Fig. 4(a), and Fig. 1(c) with Fig. 4(c)]. The similarity between experiments and simulations is remarkable especially taking into account that the initial conditions were only

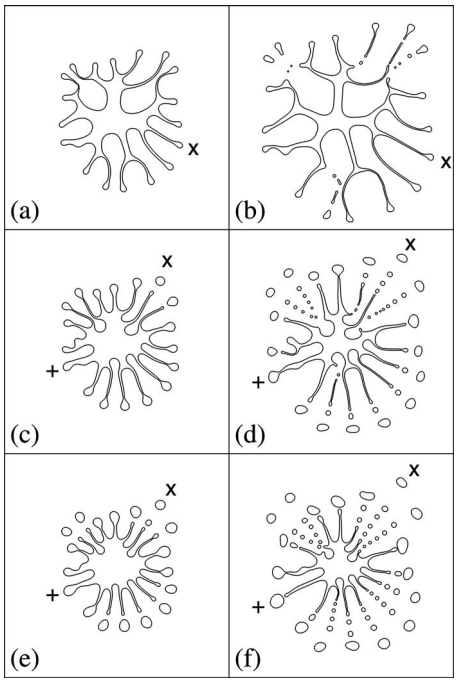


FIG. 4. Pattern evolution for a random initial condition (see text) and $B=1.03\times10^{-3}$, $\epsilon=0.005$, $dx=\epsilon$, $\tilde{\epsilon}=1$, and $A=1$ (a,b), $A=0.5$ (c,d), $A=0$ (e,f). Snapshots of size $3R_0\times3R_0$ are shown at $t=1.32$ (left) and $t=1.74$ (right).

similar. From this earlier stage it would seem that pinch-off is not significantly more present for low ($A=0.5$) than for high ($A=1$) viscosity contrast. However, the simulation offers us the possibility to go to the ideal limit $A=0$. Figure 4(e) shows that for $A=0$ most droplets have pinched off by the same time. Comparing Figs. 4(a), 4(c), and 4(e) between them, it is clear that pinch-off arises as the viscosity contrast is decreased.

At later times the experiments still show no pinch-off for $A=1$ [Fig. 1(b)], while most filaments have emitted at least one droplet for $A\simeq0.45$ [Fig. 1(d)]. The simulations would seem less conclusive, since they display some pinch-off events for $A=1$ [Fig. 4(b)]. However, these are most likely to be spurious: they occur for very narrow filaments, whose width is comparable to the interface thickness $\epsilon$. Most importantly, pinching is clearly inhibited as $\epsilon$ is decreased: the same run with a larger value of $\epsilon$ displays more pinch-off events at a given time.

Simulations for low viscosity contrasts [$A=0.5$, Fig. 4(d) and $A=0$, Fig. 4(f)] show an increasing number of pinching events as $A$ is reduced. The first pinch-off at the end of a filament does not significantly change with $\epsilon$ as will be the case for dumbbell-shaped patterns in Sec. IV C. These results already indicate that these first pinch-off events are indeed *not* spurious.

Phase-field simulations of irregular multifinger configurations from noisy perturbations of the circular interface thus confirm the tendency observed in experiments suggesting that this could not be attributed to different wetting conditions or other 3D effects. In addition, the simulations also suggest that the pinch-off events for $A=1$ are likely to be extrinsic to the 2D H-S dynamics, while those for $A<1$ are likely to be intrinsic. In the coming sections we will pursue this issue in more detail.

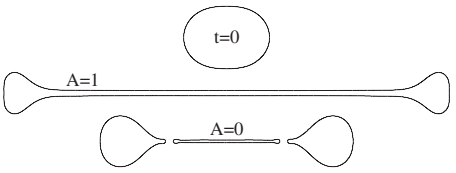


FIG. 5. Filament thinning. Top: initial condition ($n=2$, $q=0.05$). Middle and bottom: one later interface for $A=1$ and $A=0$. The other parameters are $B=0.09$, $\epsilon=0.008$, and $dx=\epsilon/2$.

### C. Intrinsic versus extrinsic pinch-off events

For simplicity and to allow direct comparison with previous studies [11,12], we first focus on the study of finite-time pinch-off by simulating the evolution of dumbbell-shaped initial conditions ($n=2$). Figure 5 displays typical patterns obtained at the end of a run ($A=1$) or just after the first pinch-off ($A=0$). In the last case secondary pinch-off events take place that give rise to satellite droplets. Figure 6 (see further discussion in Sec. IV D) shows the evolution of the filament thickness at the midpoint for the whole run ($A=1$) or up to the relaxation of the last central segment into a round shape, which makes the thickness increase again ($A=0$).

The results of our simulations are conclusive in that pinch-off events are systematically observed for low ($A=0,0.5$), but not for high ($A=0.8,1$) viscosity contrasts. This is fully consistent with experiments. Yet, the question remains as to what extent such singularities are intrinsic to the 2D H-S dynamics. One of the interesting reasons to use a

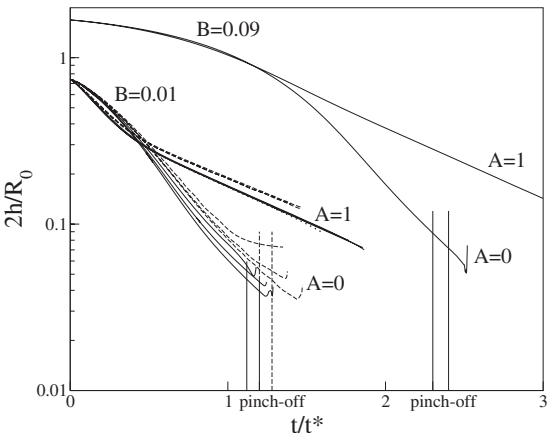


FIG. 6. Filament thinning. Width at rotation axis (in log scale) versus time. Dashed, solid, and dotted line(s): $dx=\epsilon$, $dx=\epsilon/2$, and $dx=\epsilon/4$, respectively. Upper curves ($B=0.09$): $\epsilon=0.008$ (runs in Fig. 5, $q=0.05$). Lower curves ($B=0.01$, $q=0.2$): three curves at $\epsilon=0.02$, 0.01, and 0.005 for $dx=\epsilon$ and three more at $\epsilon=0.02$, 0.01, and 0.0067 for $dx=\epsilon/2$ shown for each value of $A$. For $A=0$, lower curves correspond to lower values of $\epsilon$. The only $dx=\epsilon/4$ curve is for $A=1$, $\epsilon=0.02$. The dashed (solid) vertical lines indicate the interval during which the droplet at the tip pinches off for $dx=\epsilon(\epsilon/2)$.

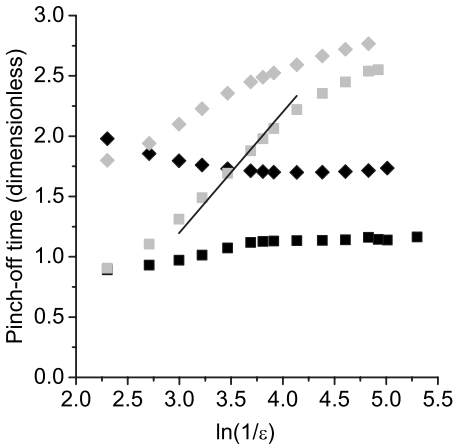


FIG. 7. Pinch-off time as a function of interface thickness $\epsilon$ in the phase-field model ($dx=\epsilon/2$, $\tilde{\epsilon}=0.5$). Black (gray) symbols represent $A=0(A=1)$. Squares correspond to dumbbells ($n=2$, and $B=0.01$, $q=0.2$) and diamonds to $n=4$ (four fingers, $B=0.0213$, $q=0.05$). In all cases, pinch-off occurs in the neck close to the advancing drop (as seen in Fig. 5) except for $A=1$, $n=2$, where it happens far away from the drop at the center of the cell. In this last case, a continuous straight line indicates the prediction explained in the text (with the theoretical slope).

phase-field approach in this respect is that the dependence on the cutoff length $\epsilon$ of the interface thickness can be used to some extent to elucidate this point. If the singularity is intrinsic, its location in time will converge with $\epsilon$ to the correct value of time, while if the time of the singularity is systematically postponed without bound, this will signal its extrinsic character at least up to the time of observation.

The dependence of pinch-off time on $\epsilon$ is analyzed in Fig. 7 for both $n=2$ and $n=4$. For $A=0$ the pinch-off time becomes practically insensitive to $\epsilon$ up to values of the interface thickness that reach beyond typical values of the experimental cutoff associated with the gap thickness in the experiments described in Sec. II B. The behavior is remarkably different for $A=1$. The pinch-off time increases monotonically as $\epsilon$ is reduced. This behavior is consistent with the spurious pinch-off associated to the finite thickness of the interface in the phase-field scheme. In fact, within the phase-field formulation, the interface pinch-off is expected to occur whenever the filament thickness reaches a threshold value of $\mathcal{O}(\epsilon)$. Accordingly, if the filament thickness decays exponentially, then the pinch-off time should scale as $(1/K')\ln(1/\epsilon)$. This prediction is roughly satisfied in the central region of the curve for $n=2$ with the theoretical value $K'=1$. Significant deviations of this prediction for smaller $\epsilon$ and for the curve $n=4$ result from additional dependence on $\epsilon$ due to the spatial shift of the pinch-off point or to deviations from the exponential scaling. The latter may originate from nonlinear orders in the lubrication approximation [Eq. (6)] from finite-$\epsilon$ corrections to the phase-field model that modify the rate of approach of the two interfaces and from effective boundary conditions enforced by the matching with the droplet (nonlubrication) region [24], when the pinch-off point is relatively close to the droplet as for $n=4$.

From this evidence we can conclude that finite-time pinch-off appears to be intrinsic to the 2D H-S dynamics for low viscosity contrast at least within the computational limitations imposed by the phase-field approach. Strictly speaking, however, we cannot rule out the possibility of changes in the pinch-off dynamics at smaller length scales similarly to the ones observed for $A=1$ for filaments thinner than $10^{-5}$ as in Refs. [11,12,24]. Such effects, if present, are likely to be irrelevant for reasonable experimental conditions, so for practical purposes, finite-time pinch-off must be considered as intrinsic for low viscosity contrast.

On the contrary, when pinch-off is observed for $A=1$, the $\epsilon$ dependence of the pinch-off time reflects the spurious nature of the singularity. Again, while this suggests that in this case the pinch-off is extrinsic, it cannot be ruled out that intrinsic singularities appear at much longer times. The phase-field approach is not appropriate to elucidate this point, but in this case, sharp-interface computations based on the lubrication approximation can be used to pursue the problem much further as reported in detail in Ref. [24]. In this case, the numerics confirms that for $A=1$, when the problem is dominated by centrifugal forces (small $B$) as in the regime studied here, finite-time singularities do not occur.

### D. Scaling of thin filaments

In Fig. 6 we see that the asymptotic decay of the filament thickness is clearly consistent with an exponential for $A=1$ as predicted by the lowest order of the lubrication approximation, although it is only observed for roughly one decade in time. For $A=0$ the filament thinning clearly deviates more from exponential. Deviations could in principle be due to the local or nonlocal next-order terms in the lubrication equation (6), but the same behavior and slopes are observed for the two different values of the dimensionless surface tension $B$ tested. That rules out the possible implication of the local term in $B$ in the range studied. This capillary term is expected to become important once a singularity is starting to build up. That could possibly happen for $A=1$ but for much larger values of $B$ [24]. Moreover, a direct observation of the interface for $A=0$ right before pinching and for $A=1$ at the same time shows that both are equally straight. The different time behavior is hence a clear signature of the nonlocal term in $1-A$ in the lubrication equation (6).

For $A=1$, the thinning rate $K'$ is well relaxed to its asymptotic value for the last third of the runs and very robust. By looking at its convergence in $\epsilon$ and $dx$ for the case $B=0.01$, we could establish it unambiguously at $K'=0.99-1.00$, in full agreement with the lowest-order prediction of the lubrication equation. For $A=0$ the relaxation is much slower and satellite drops reach the center when the rate begins to approach (from above) a value of $K'=2$. No disturbance from the previous pinch-off events is apparent. Runs for $A=0.5$ and $A=0.8$ (not shown) are also roughly consistent with a rate $K'=2/(1+A)$.

### E. Matching of filaments and droplets

In Sec. III D we have shown that an isolated circular droplet is an exact solution moving exponentially with a rate $K=1$. Furthermore, we also know that the lowest-order lubri-

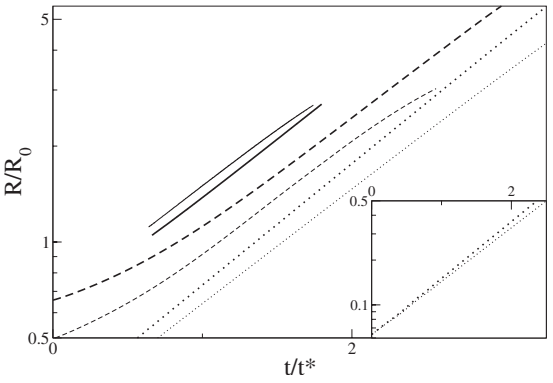


FIG. 8. Radial position (in log scale) of the center-of-mass of various droplets vs time for $A=1$ (thick) and $A=0$ (thinner curves). Solid, dashed, and dotted lines correspond to droplets indicated with an "x" in Figs. 4(a), 4(b), 4(e), and 4(f), to those in Fig. 5, and to an off-center circular droplet ($B=0.32$, $\epsilon=0.02$, $dx=\epsilon$, $\tilde{\epsilon}=0.1$, $dt=0.25\tilde{\epsilon}dx^2$), respectively. Curves are shown until the end of the respective runs, except for the isolated droplet, which is shown only up to times when finite-size effects of the simulation box are noticeable. Inset: linear regime of the isolated droplet continued in the main plot after translating the (dotted) curves to earlier times for comparison with the others. The inset preserves slopes with respect to the main plot.

cation theory yields and exponential thinning/stretching rate of $K'=2/(1+A)$. This means that for $A=1$ an isolated droplet turns out to move exponentially with precisely the same rate as the filament thinning ($K=K'$), so the filament scaling may remain essentially unaffected. More precisely, the effect of the droplet will be reduced to an appropriate boundary condition on the (local) lubrication equation [24]. On the other hand, for $A<1$ we have $K<K'$. In other words, an isolated circular droplet escapes exponentially with a rate smaller than that of the filament thinning and stretching. For $A=0$ there is a factor 2 between these two rates. This clearly signals that the picture of a constant area droplet attached to the filament works naturally for $A=1$ and not for $A<1$. In fact, mass conservation implies that the thinning of the filament must be exactly compensated by the stretching, so a droplet that does not move with the same exponential rate cannot reach a finite-area stationary shape. In this section we characterize numerically the motion of the droplets at the tip of the fingers and compare it with the motion of isolated droplets.

Figure 8 shows the evolution of the radial coordinate of a droplet center of mass for the dumbbell-shaped pattern in Fig. 5 ($n=2$, dashed lines) and for some of the outermost droplets in Fig. 4 ($n=18$, solid lines), compared to that of an isolated circular droplet ($n=1$, dotted lines). Thick (thinner) lines correspond to $A=1(0)$.

Clearly, all droplets scale with roughly the same rate $m$, although runs with $A=1$ are closer to exponential. More precisely, for $A=1(0)$, we get $m=0.8(0.7)$ for $n=2$, $m=0.82(0.75)$ for $n=18$, and $m=0.88(0.83)$ for $n=1$. Runs for $n=4$, 6, 8, 11, and 12 fingers and for intermediate values of the viscosity contrast ($A=0.5,0.8$) give similar results.

Since all droplets scale with the same rate, roughly independent of $A$ and close to $K=1$, it is clear that the droplet asymptotics is dominated by that of an isolated droplet regardless of viscosity contrast. This rate is also found to be insensitive to eventual pinch-off; in particular, a droplet which pinches off only at the end of the run (marked with "+" in Fig. 4) scales with the same rate as one of the first to pinch (marked with "x" in Fig. 4). The same rate close to $K=1$ also holds for an isolated droplet (dotted lines in Fig. 8).

In summary, a clear mismatch is observed in the simulations between the exponential rate of the droplet, always close to $K=1$ and that of the filament thinning, close to $K'=2/(1+A)$; the mismatch becomes more significant for smaller $A$. Accordingly, except for $A=1$, the droplet velocity is smaller than the filament stretching predicted by the lowest-order lubrication theory, which is forced by mass conservation to scale as the thinning of the filament. This implies that the problem for $A<1$ cannot actually be separated into two regions, one filament approaching the exponential thinning and one droplet approaching a constant area. There will typically be an excess mass injected into the droplet region. Most remarkably, although the nonlocal effects in the lubrication approximation for $A<1$ are manifest in the slight deviation from the exponential scaling, the fact that the asymptotic thinning is nevertheless approaching the one predicted by the lowest-order (local) lubrication equation defined by $K'$ (rather than adapting to $K$) is a clear indication that a singularity must build up. The occurrence of the pinch-off singularity, taking place in the regions connecting the droplet and the filament, can be seen as a consequence of the incompatibility between the lowest-order asymptotic behavior of the two regions. This provides a simple kinematic mechanism for singularity formation which would explain in simple physical terms the qualitative difference between $A=1$ and $A<1$.

## V. SUMMARY AND CONCLUSIONS

We have studied the formation of patterns that arise from a morphological instability and lead generically to the formation of thin filaments with possible generation of pinch-off singularities. Such singularities had been observed in experiments, showing a remarkable sensitivity to viscosity contrast, but the quasi-2D nature of the problem posed the question of whether and when such singularities are inherent to the 2D H-S problem (intrinsic) or due to external nonuniversal effects, related to the physics of the 3D meniscus and contact with the plates, and thus avoidable in principle (extrinsic). We have identified three different asymptotic regimes which we have studied analytically: (i) a constant mass region at rest with cusplike shapes that can be obtained exactly; (ii) a lubrication region where thin fluid filaments are formed; and (iii) an exact isolated droplet solution moving exponentially away from the cell center. This analysis has shed some light into the effect of viscosity contrast on the possible existence of finite-time singularities showing that a simple matching of the lubrication and the droplet regions that keeps the fluid filament stretching exponential (thus avoiding the buildup of singularities in finite time) is only possible for $A=1$. For $A<1$, the nonlocal effects, manifest in particular through the

mismatch between the scaling of the lowest-order lubrication approximation for the filament and the droplet behavior, are responsible for the deviation from simple exponential stretching of the filament, thus opening the way to possible singularities. These analytical arguments have been explicitly checked numerically and they provide the rationale for the interpretation of the results. Within this framework, the occurrence of singularities may be associated to a kinematic mechanism reflecting the incompatibility of the asymptotics of the two regions, the filament and the droplet, which can only be smoothly connected in the special case of $A=1$.

We have proposed to approach the problem numerically within a phase-field scheme with the idea that the introduction of a controlled cutoff length $\epsilon$ will mimic the existence of a physical cutoff in the problem, therefore allowing to elucidate the intrinsic vs extrinsic character of the singularities in terms of the sensitivity of the occurrence of the (regularized) topological singularities to that cutoff. We have obtained that the same increase in the frequency of occurrence of singularities with decreasing $A$ observed in experiments is reproduced. Furthermore, we find that the singularities for $A<1$ are likely to be intrinsic in the sense above, since the singularity time converges to a finite value with decreasing $\epsilon$. This conclusion is limited to the range of scales accessible with phase-field methods, but the fact that we have reached a certain level of analytical understanding for the mechanisms of buildup of singularities further reinforces our conclusion. On the other hand, for $A=1$, pinch-off singularities are much less frequent and when they occur they can be postponed without bound by reducing the cutoff length in the simulation. We are thus led to conclude that they are in principle extrinsic, at least for the range of parameters studied (where centrifugal forces dominate over capillary forces). Interestingly, the specificity of the $A=1$ case, for which the lubrication approximation is local, allows a complementary study within the usual sharp-interface methods to properly elucidate the competition between centrifugal and capillary forces in general. This is done in the complementary paper [24], where it is shown that intrinsic singularities may be present for other parameter regimes in the case $A=1$ but are not present in the regime studied here. Interestingly, the case where the phase-field approach is less conclusive ($A=1$) is precisely the one best adapted to the sharp-interface/lubrication methods, while the cases where sharp-interface methods become particularly involved ($A<1$) are those for which the phase-field approach is most conclusive. From a practical point of view, we would like to stress that the actual values of the phase-field cutoff reached in our simulations are comparable or even smaller than reasonable values of cell-gap cutoff in realistic experiments. Accordingly, with the necessary word of caution regarding a proper mathematical statement on the existence of finite-time singularities, our results are indeed conclusive for many practical purposes. From a theoretical point of view, it remains an open question not only the strict proof of existence of singularities but also the degree of universality of their mathematical structure. While the evidence for $A=1$ when capillary forces dominate points out to a strong sensitivity to initial conditions and history [11,12,24], with low degree of universality, singularities generated by centrifugal forcing for low viscosity contrast seem to be rather robust. In particular, the existence of a kinematic mechanism for singularity formation may be suggestive of a more universal character of them.

## ACKNOWLEDGMENTS

We are grateful to Jens Eggers, Raymond Goldstein, and Michael Siegel for illuminating discussions. R.F. and E.A.-L. acknowledge a Ramón y Cajal and a Juan de la Cierva grant from MICINN, Spain, respectively. Financial support from Ministerio de Ciencia e Innovación (MICINN, Spain) under Projects No. FIS2006-03525 and No. CTQ2008-06469/PPQ, from Generalitat de Catalunya under Projects No. 2005-SGR-507 and No. 2009-SGR-14, from European Commission under Project No. HPRN-CT-2002-00312, and from Universitat Rovira i Virgili under Project No. 2006AIRE-01 is acknowledged.

[1] J. Eggers, Rev. Mod. Phys. **69**, 865 (1997).
[2] M. Moseler and U. Landman, Science **289**, 1165 (2000).
[3] J. Eggers, Phys. Rev. Lett. **89**, 084502 (2002).
[4] A. Oron, S. H. Davis, and S. G. Bankoff, Rev. Mod. Phys. **69**, 931 (1997).
[5] S. Tanveer and G. L. Vasconcelos, Phys. Rev. Lett. **73**, 2845 (1994).
[6] R. E. Goldstein, A. I. Pesci, and M. J. Shelley, Phys. Rev. Lett. **70**, 3043 (1993).
[7] T. F. Dupont, R. E. Goldstein, L. P. Kadanoff, and S.-M. Zhou, Phys. Rev. E **47**, 4182 (1993).
[8] P. Constantin, T. F. Dupont, R. E. Goldstein, L. P. Kadanoff, M. J. Shelley, and S.-M. Zhou, Phys. Rev. E **47**, 4169 (1993).
[9] R. E. Goldstein, A. I. Pesci, and M. J. Shelley, Phys. Rev. Lett. **75**, 3665 (1995).
[10] R. E. Goldstein, A. I. Pesci, and M. J. Shelley, Phys. Fluids **10**, 2701 (1998).
[11] R. Almgren, Phys. Fluids **8**, 344 (1996).
[12] R. Almgren, A. Bertozzi, and M. Brenner, Phys. Fluids **8**, 1356 (1996).
[13] P. G. Saffman and G. I. Taylor, Proc. R. Soc. London, Ser. A **245**, 312 (1958).
[14] D. Bensimon, L. P. Kadanoff, S. Liang, B. I. Schraiman, and C. Tang, Rev. Mod. Phys. **58**, 977 (1986).
[15] G. Tryggvason and H. Aref, J. Fluid Mech. **154**, 287 (1985).
[16] J. Casademunt, Chaos **14**, 809 (2004).
[17] L. Carrillo, F. X. Magdaleno, J. Casademunt, and J. Ortín, Phys. Rev. E **54**, 6260 (1996).
[18] E. Alvarez-Lacalle, E. Pauné, J. Casademunt, and J. Ortín, Phys. Rev. E **68**, 026308 (2003).
[19] E. Alvarez-Lacalle, J. Ortín, and J. Casademunt, Phys. Fluids **16**, 908 (2004).
[20] J. A. Miranda and E. Alvarez-Lacalle, Phys. Rev. E **72**, 026306 (2005).

[21] J. V. Maher, Phys. Rev. Lett. **54**, 1498 (1985).
[22] J. Casademunt and D. Jasnow, Phys. Rev. Lett. **67**, 3677 (1991).
[23] A. Sierou and J. R. Lister, J. Fluid Mech. **497**, 381 (2003).
[24] E. Alvarez-Lacalle, J. Casademunt, and J. Eggers, following paper, Phys. Rev. E **80**, 056306 (2009).
[25] W. J. Boettinger, J. A. Warren, C. Beckermann, and A. Karma, Annu. Rev. Mater. Res. **32**, 163 (2002).
[26] L.-Q. Chen, Annu. Rev. Mater. Res. **32**, 113 (2002).
[27] R. González-Cinca, R. Folch, R. Benítez, L. Ramírez-Piscina, J. Casademunt, and A. Hernández-Machado, in *Advances in Condensed Matter and Statistical Physics*, edited by E. Korutcheva and R. Cuerno (Nova Science, New York, 2004), pp. 203–236.
[28] R. Folch, J. Casademunt, A. Hernández-Machado, and L. Ramírez-Piscina, Phys. Rev. E **60**, 1724 (1999).
[29] R. Folch, J. Casademunt, A. Hernández-Machado, and L. Ramírez-Piscina, Phys. Rev. E **60**, 1734 (1999).
[30] R. Folch, J. Casademunt, and A. Hernández-Machado, Phys. Rev. E **61**, 6632 (2000).
[31] E. Alvarez-Lacalle, J. Ortín, and J. Casademunt, Phys. Rev. E **74**, 025302(R) (2006).
[32] E. Pauné, Ph.D. thesis, Universitat de Barcelona, 2002 (available at http://www.tdx.cat/TDX-0123103-115958).
[33] The fingers of the outer (less viscous) fluid penetrating toward the cell center exhibit competition. Some of them, thus, stop at larger radial distances than others. This explains the apparent bifurcation of some of the outgoing fingers, which should not be mistaken for a tip-splitting instability of the outward fingers.
[34] E. Alvarez-Lacalle, J. Ortín, and J. Casademunt, Phys. Rev. Lett. **92**, 054501 (2004).
[35] Note that this term can be constructed from the case with gravity discussed in [10], now for a gravity that grows linearly with $x$.
[36] F. X. Magdaleno, Ph.D. thesis, Universitat de Barcelona, 2000.